Electronic structure of $MoSe_2$, MoS_2, and WSe_2. II. The nature of the optical band gaps

R. Coehoorn* and C. Haas
Laboratories of Physical and Inorganic Chemistry, Materials Science Centre of the University of Groningen, Nijenborgh 16, 9747 AG Groningen, The Netherlands

R. A. de Groot
Research Institute for Materials, Faculty of Science, University of Nijmegen, Toernooiveld, 6515 ED Nijmegen, The Netherlands
(Received 20 October 1986)

From band-structure calculations it is shown that $MoSe_2$, MoS_2, and WSe_2 are indirect-gap semiconductors. The top of the valence band is at the Γ point and the bottom of the conduction band is along the line T of the hexagonal Brillouin zone, halfway between the points Γ and K. The A and B excitons correspond to the smallest direct gap at the K point. This assignment of the exciton peaks is shown to be consistent with the polarization dependence of their intensities, their effective masses, and the observed dependence of their splitting on the spin-orbit splittings of the constituent elements. The wave function at the top of the valence band is shown to be a metal-nonmetal antibonding state, which explains the observed high stability of these materials in photoelectrochemical cells against photocorrosion.

I. INTRODUCTION

In the preceding paper,[1] referred to in the following as I, we presented band-structure calculations of the semiconducting layered compounds $MoSe_2$, MoS_2, and WSe_2, and photoelectron spectroscopy measurements of $MoSe_2$. In agreement with measurements of the optical spectra[2,3] and early (two-dimensional, non-self-consistent) band-structure calculations,[4] it was shown that their electronic structures are very similar. Furthermore, the self-consistent calculated band structures in I show that the optical band gaps are indirect, in agreement with non-self-consistent band-structure calculations of MoS_2 (Refs. 5–9) and photocurrent measurements in an electrochemical cell.[10]

In this paper the nature of the indirect and direct gaps is discussed. In some band-structure calculations[5,9] the top of the valence band was situated at Γ, while in other calculations[6–8] only a very small (and probably insignificant) difference between the position of the highest occupied bands at Γ and K was found. In Secs. II and III it is shown from band-structure calculations and photoelectron spectroscopy, respectively, that the top of the valence band is situated at Γ.

The nature of the direct gaps has been investigated by studying the exciton pair just below the main absorption edge. The energies and distances of these so-called A and B excitons are given in Table I, including the data for $MoTe_2$ and MoS_2. Following Wilson and Yoffe[2] many authors have attributed the A-B exciton pair to transitions at Γ, split by spin-orbit splitting, as suggested by the dependence of the splittings on the masses of the constituent elements. Indeed, in some calculated band structures the smallest direct gap is situated at Γ,[5,9] but other calculations yielded a direct gap at K.[6–8] Up to now the locations in the Brillouin zone of the direct gap, and of the transitions to which the A-B excitons belong have been a point of debate. In Sec. IV it is shown that the A and B excitons correspond to the smallest direct transitions at the K point of the Brillouin zone.

Section V contains some remarks about the relevance of this work for the application of molybdenum and tungsten dichalcogenides in electrochemical solar cells.

TABLE I. Energy of excitons in Mo and W dichalcogenides. If a Rydberg series is observed, the energy of the $n=1$ peak is tabulated. These values are from Ref. 3. In Refs. 2 and 17 slightly different energies are given.

	$E(A)$ (eV)	$E(B)$ (eV)	$E(B)-E(A)$ (eV)
$2H$-MoS_2	1.88	2.06	0.18
$2H$-$MoSe_2$	1.57	1.82	0.25
$2H$-$MoTe_2$	1.10	1.48	0.38
$3R$-WS_2	2.06	2.50	0.44
$2H$-WSe_2	1.71	2.30	0.59

II. BAND-STRUCTURE CALCULATIONS

From the calculated augmented-spherical-wave (ASW) band-structure calculations, presented in I, it can be concluded that in $MoSe_2$, MoS_2 and WSe_2 the top of the valence band is situated at Γ, the bottom of the conduction band is situated on the line T, halfway between Γ and K, and that the direct gap is situated at the K point. In Table II the character of the wave function of the most important states near the band gaps are given by $MoSe_2$. The Γ_4 state at the top of the valence band is of mixed Mo d—Se p character, as already found experimentally by electron paramagnetic resonance experiments.[11]

The experimental indirect gaps of $MoSe_2$, MoS_2, and

TABLE II. Contributions from the basis functions to the wave functions of some states near the top of the valence band and the bottom of the conduction band of $MoSe_2$. Only contributions larger than 1% are tabulated. Note that the tabulated numbers depend on the size of the Wigner-Seitz spheres.

Energy (eV)	Symmetry	
0.00[a]	Γ_4^-	3% Mo s + 57% Mo d_{z^2} + 5% Se s + 35% Se p_z
1.10[b]		38% $\frac{1}{2}$Mo d_{xy} + (Mo $d_{x^2-y^2}$) + (9% Mo d_{z^2} + 4% Se s + 26% $\frac{1}{2}$Se p_x + (Se p_y) + 9% (Se d_{xz} + Se d_{yz}) + 5% (Se d_{xy} + Se $d_{x^2-y^2}$)
−0.81	K_1	42% Mo d_{xy} + 42% Mo $d_{x^2-y^2}$ + 5% Se p_x + 5% Se p_y
−0.55	K_4	41% Mo d_{xy} + 41% Mo $d_{x^2-y^2}$ + 8% Se p_x + 8% Se p_y
1.35	K_5	5% Mo s + 77% Mo d_{z^2} + 6% Se p_y + 6% Se p_x 5% Mo s + 77% Mo d_{z^2} + 6% Se p_y + 6% Se p_x
1.55	K_2	21% Mo d_{xz} + 21% Mo d_{yz} + 9% Se p_y + 9% Se p_x + 4% Se d_{xy} + 15% Se d_{yz} + 15% Se d_{xz} + 4% Se $d_{x^2-y^2}$

[a]Top valence band.
[b]Bottom conduction band at $|\mathbf{k}| = 0.55\Gamma K$.

WSe_2 are 1.1, 1.2, and 1.2 eV, respectively.[10,12] These values are much larger than the calculated gaps (0.35 eV for $MoSe_2$). This discrepancy is a systematic feature of the local density approximation in band-structure calculations.[13] Generally the calculated gaps are 30—50% too small. For $MoSe_2$ a good agreement with the experimental indirect gap can be obtained by a rigid shift of 0.75 eV of the conduction bands with respect to the valence bands. In our view the A-B exciton peaks near the absorption edge belong to $K_4 \rightarrow K_5$ and $K_1 \rightarrow K_5$ optical transitions. If we assume that the binding energy of the A exciton is about 0.05 eV, the experimental direct gap for $MoSe_2$ is about 1.6 eV. This value is within its accuracy equal to the energy difference of 1.6 eV between the K_5 state shifted by + 0.75 eV to 1.35 eV, and the experimental position of the K_4 state at −0.25 eV (as found from photoelectron spectroscopy, see Sec. III).

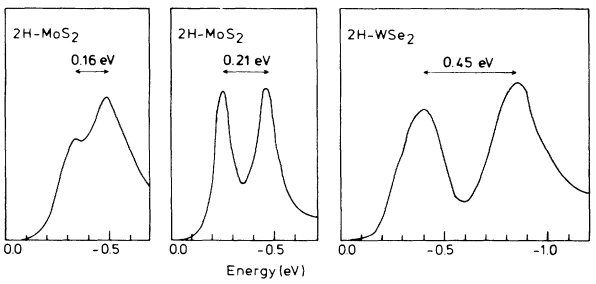

FIG. 1. HeI ARUPS spectra at the $K(H)$ point of the Brillouin zone, for MoS_2, $MoSe_2$, and WSe_2, with angle of light incidence $\alpha = 45°$. The energy is with respect to the top of the valence band at Γ.

III. ANGLE-RESOLVED ULTRAVIOLET PHOTOELECTRON SPECTROSCOPY (ARUPS)

In I it was shown for $MoSe_2$ that the band-structure calculations give a very good description of the electronic structure of the occupied states. Due to the close resemblance of their electronic structures, we expect that this will also be true for MoS_2 and WSe_2.

In Fig. 1 high-resolution (FWHM of 0.02 eV) ARUPS spectra are shown of the upper valence bands of MoS_2, $MoSe_2$, and WSe_2 at the $K(H)$ points in the Brillouin zone. The spectra show two peaks, split by 0.16, 0.21, and 0.45 eV, respectively. Within the experimental resolution, ARUPS measurements using synchrotron radiation in the range 19 eV $\leqq h\nu \leqq$ 31 eV show that the peak positions are photon-energy independent.[14] We ascribe the peaks to the K_1 and K_4 critical points. These measurements show in a very direct way that the top of the valence band is located at Γ, and not at K.

IV. THE A AND B EXCITON PEAKS

The A and B exciton peaks near the optical-absorption edge are a characteristic feature of the optical spectra of all layered molybdenum and tungsten dichalcogenides.[2] We assign these excitons to transitions at the K point, with K_1 and K_4 as initial states, and the K_5 state as the final state. In this section we show that the experimental data, analyzed with the help of ASW band-structure calculations, support this assignment.

$K_1 \rightarrow K_5$ and $K_4 \rightarrow K_5$ transitions are allowed with x,y polarized light (in the a-b plane) and forbidden for z polarized light.[15] Such a polarization dependence of the exciton peak intensities is indeed observed.[16] From dipole selection rules it follows that the K_2 state, which lies close to the K_5 state, cannot be the final state for transitions

from K_1 and K_4 states if x,y polarized light is used.

Other evidence for the correctness of this assignment comes from the observed exciton effective masses. The excitons can be described as three-dimensional Wannier excitons.[17] For the case of MoS_2 Evans[17] has estimated the exciton effective masses from the $n=1$—4 terms of the Rydberg series of A and B excitons:

$$\mu_{||}^{A}=1.28m_0\ ,\quad \mu_{||}^{B}=4.10m_0\ ,$$
$$\mu_{\perp}^{A}=0.31m_0\ ,\quad \mu_{\perp}^{B}=0.99m_0\ , \tag{1}$$

in which m_0 is the free-electron mass, and in which the $||$ and $\perp$ directions are parallel and normal to the c axis. Using the relations

$$\frac{1}{\mu_{||}}=\frac{1}{m_e^{||}}+\frac{1}{m_h^{||}}\ \text{and}\ \frac{1}{\mu_{\perp}}=\frac{1}{m_e^{\perp}}+\frac{1}{m_h^{\perp}}\ , \tag{2}$$

where m_e and m_h are the electron and hole effective masses, the exciton effective masses can be derived from the ASW band-structure calculations. The calculated parallel effective masses are

$$\mu_{||}(K_4-K_5)=0.9m_0\ ,$$
$$\mu_{||}(K_1-K_5)=3.2m_0\ . \tag{3}$$

These values are close to the experimental values of $\mu_{||}^{A}$ and $\mu_{||}^{B}$. The masses depend on the K_1-K_4 splitting. The values in (3) are derived from a scalar relativistic calculation, with a K_1-K_4 splitting of 0.23 eV. A calculation of the perpendicular masses is not so straightforward, because along ΓK the electron band that originates from K_5 splits into two nonparabolic bands. Very close to K_5 the masses $m_{\perp}(K_5)$ are $0.4m_0$ and $0.9m_0$. For the K_1 and K_4 states, the perpendicular masses are $m_{\perp}=0.8m_0$. These data explain why $\mu_{\perp}^{A}$ as well as $\mu_{\perp}^{B}$ are smaller than $\mu_{||}^{A}$ and $\mu_{||}^{B}$. From the calculations it is not clear why $\mu_{\perp}^{B}$ is much larger than $\mu_{\perp}^{A}$. Finally we remark that the calculated hole mass for the Γ_4^- state at the top of the valence band is $m_{||}=0.9m_0$. This value is far too small to explain the high effective parallel mass of the B exciton if it were located at Γ, indicating again that the AB excitons are not at Γ.

Now we look more closely at the energy difference of the A and B excitons (Table I). Due to the dependence of their splitting on the mass of the constituent atoms, these peaks were generally assumed to be a spin-orbit-split pair. In Fig. 2 a model calculation of the effect of spin-orbit splitting on the conduction-band structure at Γ is presented. Starting from the scalar relativistic band structure of $MoSe_2$, spin-orbit interaction of metal d states and nonmetal p states was included as a perturbation (see I). The two middle parts of the figure show the unoccupied states as a function of λ_d, with $\lambda_p=0$, and as a function of λ_p, with $\lambda_d=0$. The atomic $(d_{3/2}-d_{5/2})$ spin-orbit splitting is $\frac{5}{2}\lambda_d$, and the atomic $(p_{1/2}-p_{3/2})$ spin-orbit splitting is $\frac{3}{2}\lambda_p$. In the two outer parts of the figure the unoccupied states are given as a function of λ_p, with $\frac{5}{2}\lambda_d$ fixed at 0.275 eV (the value for Mo), and as a function of λ_d, with $\frac{3}{2}\lambda_p$ fixed at 0.42 eV (the value for Se). In the absence of spin-orbit interaction $\Gamma_4^-\rightarrow\Gamma_5^+$ is the only allowed transition from the top of the valence band to the conduction band. From Fig. 2 it can easily be seen that the A-B excitons are not located at Γ:

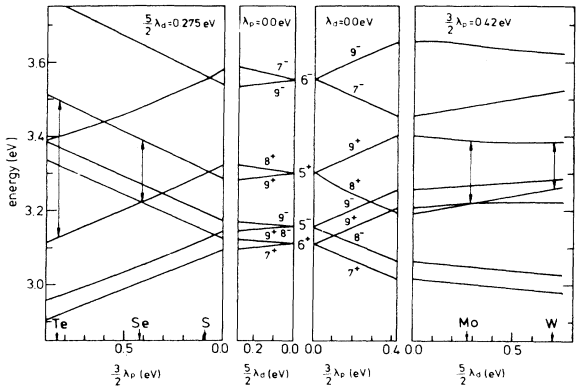

FIG. 2. Effect of spin-orbit interaction on the band structure of $MoSe_2$ at Γ. Energy scale with respect to the top of the valence band, shifted upward by 0.75 eV (see Sec. II).

(i) The calculated $\Gamma_4^-\rightarrow\Gamma_5^+$ energy difference is much higher than the experimental A and B exciton energies (3.3 eV versus 1.57 and 1.82 eV, respectively).

(ii) The $\Gamma_5^+\rightarrow\Gamma_9^+ + \Gamma_8^+$ spin-orbit splitting due to the metal d and nonmetal p contributions to the wave functions have different signs, and the metal d contribution to these states is rather small (20%). The calculated trends in the splittings (arrows in Fig. 2) are in complete disagreement with the observed A-B exciton splittings (Table I).

The results of a similar model calculation of the effect of spin-orbit splitting of the band structure at K are given in Fig. 3. The calculated contribution of the metal d spin-orbit interaction is of the right sign and magnitude. The contribution of the nonmetal p spin-orbit interaction on the K_1-K_4 splitting is quite small, due to the small amount of chalcogenide character in these states (see Table II).

The A-B exciton splitting is smaller than the K_1-K_4

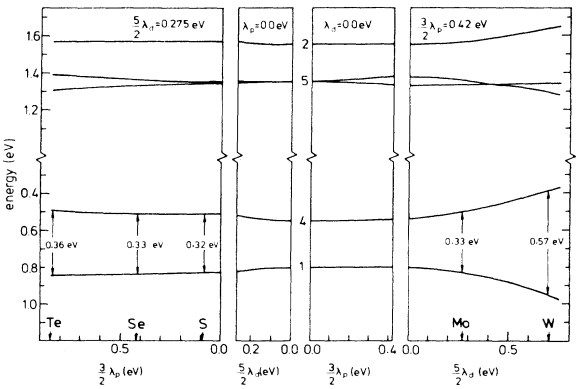

FIG. 3. Effect of spin-orbit interaction on the band structure of $MoSe_2$ at K. Energy scale with respect to the top of the valence band, shifted upward by 0.75 eV.

splitting owing to the different exciton binding energies. For MoS_2 the $n=1-4$ terms of a Rydberg series of A and B excitons obey the following relation:[17]

$$E_h^A = 1.971 - 0.042/n^2 \text{ (eV)}, \quad E_h^B = 2.267 - 0.134/n^2 \text{ (eV)}. \tag{4}$$

The experimental K_1-K_4 distance (0.296 eV) is in good agreement with the theoretical value (0.31 eV) from a fully relativistic ASW calculation of MoS_2. Note that the peak splitting in the ARUPS spectra at the $K(H)$ point (Fig. 1) is much lower (0.16 eV). For $MoSe_2$ and WSe_2, too, the ARUPS peak splitting is lower than the exciton splitting, and therefore certainly lower than the K_1-K_4 distance. An explanation for this difference is that the angle-resolved ultraviolet photoelectron spectroscopy (ARUPS) spectra can be regarded as a one-dimensional density of states (ODDOS) of the band structure along the KH line, broadened by lifetime, thermal, and instrumental effects. Such a ODDOS-like shape of the ARUPS spectra is expected if the photoelectron escape depth is of the order of the lattice parameter normal to the surface.[18] This model is supported by the observed independence of the peak positions on the photon energy (see Sec. III). Due to the broadening of the asymmetric peaks at both ends of the ODDOS, the observed peak splitting is lower than the K_1-K_4 separation. It would be interesting to look for a unified picture of the photoemission process, which should explain why the direct transition model can be applied for normal emission (I), the ODDOS model being better for emission from the $K(H)$ point.

V. CONCLUDING REMARKS

It was shown that MoS_2, $MoSe_2$, and WSe_2 are indirect gap semiconductors, with the top of the valence band at Γ and the bottom of the conduction band halfway between Γ and K. The A and B excitons correspond to the smallest direct gap at the K point. The A-B exciton splitting is due to interlayer interactions and spin-orbit splitting.

Molybdenum and tungsten dichalogenide layered compounds have possible applications as electrode materials in photoelectrochemical solar cells, as suggested first by Tributsch.[19] These cells have a high light to electrical energy conversion efficiency and are fairly stable against photocorrosion in solutions of several redox systems, if the surface is prepared carefully.[10,20] Moreover, the energy gaps of these materials match the solar spectrum very well. The stability of these materials was attributed to the fact that the optical transitions are between nonbonding metal d states.[19] The most stable hole states in semiconductors with valence bands based on p orbitals (e.g., CdS, ZnO, GaAs) are cation-anion bonding orbitals. Excitation of electrons from these states leads to photocorrosion of the electrode surface. From our band-structure calculations it is found that in the molybdenum and tungsten dichalcogenides the Γ_4^- state at the top of the valence band is not a *nonbonding* metal d state, but rather an *antibonding* state between metal d_{z^2} and nonmetal p_z orbitals. This explains the high stability of these materials against photocorrosion. The corresponding *bonding* Γ_4^- metal-d_{z^2}–nonmetal-p_z state is situated at about 5 eV below the top of the valence band. This large energy difference is an indication of the large covalent interaction between the metal d_{z^2} and nonmetal p_z orbitals.

Finally, we note that our assignment of the exciton peaks to transitions at the K point requires an entirely new discussion of the magnetic circular dichroism measurements on the exciton peaks.[21]

ACKNOWLEDGMENTS

We would like to thank R. Tenne and A. Wold for providing us with $MoSe_2$ and WSe_2 single crystals. This investigation was supported in part by the Stichting Scheikundig Onderzoek Nederland (SON) and the Stichting Fundamenteel Onderzoek van de Materie (FOM).

*Present address: Philips Research Laboratories, P.O. Box 80.000, 5600 JA Eindhoven, The Netherlands.

[1]R. Coehoorn, C. Haas, J. Dijkstra, C. J. F. Flipse, R. A. de Groot, and A. Wold, preceding paper, Phys. Rev. B **35**, 6195 (1987).
[2]J. A. Wilson and A. D. Yoffe, Adv. Phys. **18**, 193 (1969).
[3]A. R. Beal, W. Y. Liang, and H. P. Hughes, J. Phys. C **9**, 2449 (1976); A. R. Beal, and H. P. Hughes, J. Phys. C **12**, 881 (1979).
[4]R. A. Bromley, R. B. Murray, and A. D. Yoffe, J. Phys. C **5**, 759 (1972).
[5]R. V. Kasowski, Phys. Rev. Lett. **30**, 1175 (1973).
[6]L. F. Matheiss, Phys. Rev. Lett. **30**, 784 (1973); Phys. Rev. B **8**, 3719 (1973).
[7]K. Wood and J. B. Pendry, Phys. Rev. Lett. **31**, 1400 (1973).
[8]S. P. Hind and P. M. Lee, J. Phys. C **13**, 349 (1980).
[9]D. W. Bullett, J. Phys. C **11**, 4501 (1978).
[10]K. K. Kam and B. Parkinson, J. Phys. Chem. **86**, 463 (1982).
[11]R. M. M. Fonville, W. Geertsma, and C. Haas, Phys. Status Solidi B **85**, 621 (1978).
[12]K. K. Kam, C. L. Chang, and D. W. Lynch, J. Phys. C **17**, 4031 (1984).
[13]J. P. Perdew and A. Zunger, Phys. Rev. B **23**, 5048 (1981); J. P. Perdew and M. Levy, Phys. Rev. Lett. **51**, 1884 (1983).
[14]R. Coehoorn, thesis, University of Groningen, 1985.
[15]M. Schlüter, in *Electrons and Phonons in Layered Crystal Structures,* edited by T. J. Wieting and M. Schlüter (Riedel, Dordrecht, 1979), p. 29. For a note on the symmetry notation used in our band-structure plots, see Ref. 1, Sec. II B.
[16]W. Y. Liang, J. Phys. C **6**, 551 (1973).
[17]B. L. Evans, in *Optical and Electrical Properties,* Vol. 4 of *Physics and Chemistry of Materials with Layered Structures,* edited by P. A. Lee (Riedel, Dordrecht, 1976), p. 1.
[18]F. Minami, M. Sekita, N. Aono, and N. Tsuda, Solid State Commun. **29**, 459 (1974).
[19]H. Tributsch, Z. Naturforsch. **32a**, 972 (1977).
[20]W. Kautek, H. Gerischer and H. Tributsch, J. Electrochem. **127**, 2471 (1980).
[21]M. Tanaka, G. Kuwabara, and H. Fukutani, J. Phys. Soc. Jpn. **51**, 3888 (1982).